Mesoscopic dynamics of Voronoi fluid particles

2002 J. Phys. A: Math. Gen. 35 1605

(http://iopscience.iop.org/0305-4470/35/7/310)

INSTITUTE OF PHYSICS PUBLISHING JOURNAL OF PHYSICS A: MATHEMATICAL AND GENERAL

J. Phys. A: Math. Gen. **35** (2002) 1605–1625 PII: S0305-4470(02)28700-4

Mesoscopic dynamics of Voronoi fluid particles

Mar Serrano[1], Gianni De Fabritiis[2], Pep Español[1], Eirik G Flekkøy[3] and Peter V Coveney[2]

[1] Departamento de Física Fundamental, UNED, Apartado 60141, 28080 Madrid, Spain
[2] Centre for Computational Science, Queen Mary, University of London, Mile End Road, London E1 4NS, UK
[3] Department of Physics, University of Oslo, PO Box 1048 Blindern, 0316 Oslo 3, Norway

Received 6 September 2001, in final form 3 December 2001
Published 8 February 2002
Online at stacks.iop.org/JPhysA/35/1605

Abstract

We compare and contrast two recently reported mesoscopic fluid particle models based on a two-dimensional Voronoi tessellation. Both models describe a Newtonian fluid at mesoscopic scales where fluctuations are important. From the requirement of thermodynamic consistency, the equilibrium distribution function is given through the Einstein distribution function. We compute from the Einstein distribution the equilibrium distribution function for a single fluid particle. We observe excellent agreement between the simulation results for the proposed models and the theoretical distribution function.

PACS numbers: 47.10.+g, 05.20.−y

(Some figures in this article are in colour only in the electronic version)

1. Introduction

The dynamical regimes of complex fluids such as colloidal suspensions or polymeric solutions are strongly affected by the fluctuating character of the solvent. The Brownian diffusive character of small suspended objects can be traced back to the stochastic nature of the surrounding fluid [1]. Mathematically, the equations of the fluctuating hydrodynamics (FH) [2] model in the continuum limit the *mesoscopic* regime of a simple Newtonian fluid. This regime corresponds to small length scales where, although the fluid is still well represented by hydrodynamics (a kinetic description is not yet needed), the molecular nature of the fluid is already appreciable and it is modelled through the inclusion of random noise terms in the hydrodynamic equations. The noise appears as the divergence of a random stress tensor and random heat flux, and the structure of these random fluxes is entirely determined from the fluctuation–dissipation theorem [2, 3]. The mesoscopic regime of hydrodynamics is relevant not only in problems involving complex fluids, but also in simple fluids when probed at short-length scales, as, for example, in light scattering experiments.

A simulation of a fluid at mesoscopic scales could be based on a discretization of the fluctuating hydrodynamic equations which, however, requires some care [4]. One should introduce the discrete random terms in such a way that they are compatible with the discrete form of the dissipation in the equations, in strict respect of the fluctuation–dissipation theorem even at the discrete level. Only in this way does one expect to have the Einstein distribution for mesoscopic variables as the equilibrium distribution function. Also, one should be careful in selecting thermal fluctuations with respect to conservation of mass, momentum and energy.

Recently, two models have been devised and implemented in order to simulate fluctuating hydrodynamics [5, 6]. Both are based on a dynamical Voronoi Lagrangian grid that follows the flow field. The main differences between both models are the use of entropy or energy as an independent variable and, more importantly, how the velocity and temperature gradients are discretized. From a methodological point of view, we use different though equivalent and complementary ways of obtaining the stochastic forces in order to fulfil the fluctuation–dissipation theorem. The first approach [5, 7] consists in writing the equilibrium distribution for the set of variables, guessing the structure of the random noise, computing the Fokker–Planck operator acting equation corresponding to the Langevin equations and deriving the coefficients of the noise by balancing the diffusive and drift parts of the Fokker–Planck operator acting on the equilibrium distribution. The second approach uses the GENERIC formalism [6, 8]. GENERIC is a very general framework for non-equilibrium thermodynamics which encodes in a very simple way the physics behind the first and second laws of thermodynamics *and* the fluctuation–dissipation theorem. It must be emphasized that the GENERIC formalism does not include any new physics, but permits one to rapidly identify whether or not a model is thermodynamically consistent and, if it is not, offers suggestions on how to restore thermodynamic consistency. The model in [6] produces results of higher numerical accuracy than the model in [5]. This is because the evaluation of gradients, using both nearest and next-nearest neighbour data, is more precise in the former model. In the latter model, however, interactions are strictly local in the sense that only nearest-neighbour interactions take place. This feature brings the latter model closer to existing DPD models [9, 10], and it may prove useful in applications where interaction forces other than those within a simple Newtonian fluid are included.

In section 2 we review both models, discussing their similarities and differences. We show that the reversible part of the dynamics of the model in [5] has a tiny production of entropy, but it can be easily modified in order to have a zero production of entropy as corresponds to a purely reversible dynamics. We also show in an appendix that the irreversible part of the dynamics of the model in [5] can be cast in the GENERIC formalism thus ensuring a positive entropy production. In section 3 we discuss how one can derive from the N-particle Einstein distribution function the one-particle distribution function, which is the object measurable in simulations. This allows one to discuss the validity of the models in order to simulate fluctuating hydrodynamics.

2. The models

The models in [5, 6] can be understood as discretized versions of the continuum equations of fluctuating hydrodynamics in terms of fluid particles that move following the flow. The advantage of a Lagrangian description is apparent when one thinks of the highly complex and evolving interstitial domains in a colloidal suspension where the solvent fluid evolves. The fluid particles have definite positions $\boldsymbol{R}_i$ and have associated a region of space around each given by its Voronoi cell. Each cell is defined as the region of space closer to the centre of that cell than to any other cell centre. This produces a partition of physical space into a set

of non-overlapping regions, the so called Voronoi tessellation. Each cell can be regarded as a thermodynamic subsystem of the whole fluid system and is associated with a mass M_i, a momentum $\boldsymbol{P}_i$ and an internal energy $\mathcal{E}_i$, which can be defined in microscopic terms from the momenta and coordinates of the molecules that constitute the fluid [5]. The cells also have a specified volume $\mathcal{V}_i$, which is a geometrical quantity dependent on the coordinates of the cell centres, and an entropy function S_i, which is a prescribed thermodynamic function of the extensive variables $M_i, \mathcal{E}_i, \mathcal{V}_i$. We will refer to the fluid particles defined in terms of the Voronoi cells as *mesoparticles*.

The equations of motion for the mesoscopic variables have been obtained either from molecular considerations [5] plus simple finite difference approximation of velocity gradients, or from a finite volume discretization of the Navier–Stokes equations [6]. We discuss the connections and differences between these two models by separating the equations of motion into their reversible and irreversible parts.

2.1. Reversible part

The evolution equations of an inviscid fluid are completely reversible. By selecting as independent state variables the position, mass, momentum and entropy $\boldsymbol{R}_i, M_i, \boldsymbol{P}_i, S_i$, for $i = 1, \ldots, N$, the reversible part of the dynamics of a discrete model for an inviscid fluid is given by [6]

$$\begin{aligned}
\dot{\boldsymbol{R}}_i &= \boldsymbol{v}_i \\
\dot{\boldsymbol{P}}_i &= \sum_j A_{ij}\boldsymbol{e}_{ij}\frac{P_j - P_i}{2} + \sum_j \frac{A_{ij}}{R_{ij}}\frac{\rho_i + \rho_j}{2}\frac{\boldsymbol{v}_i + \boldsymbol{v}_j}{2}\boldsymbol{c}_{ij}\cdot\boldsymbol{v}_{ij} \\
&\qquad + \sum_j \frac{A_{ij}}{R_{ij}}\boldsymbol{c}_{ij}\left((P_i - P_j) - \frac{\rho_i + \rho_j}{2}(\mu_i - \mu_j) - \frac{s_i + s_j}{2}(T_i - T_j)\right) \qquad (1) \\
\dot{M}_i &= \sum_j \frac{A_{ij}}{R_{ij}}\frac{\rho_i + \rho_j}{2}\boldsymbol{c}_{ij}\cdot\boldsymbol{v}_{ij} \\
\dot{S}_i &= \sum_j \frac{A_{ij}}{R_{ij}}\frac{s_i + s_j}{2}\boldsymbol{c}_{ij}\cdot\boldsymbol{v}_{ij}.
\end{aligned}$$

Here, $\boldsymbol{v}_i = \boldsymbol{P}_i/M_i$ is the velocity ($\boldsymbol{v}_{ij} = \boldsymbol{v}_i - \boldsymbol{v}_j$), $\rho_i = M_i/\mathcal{V}_i$ is the mass density and $s_i = S_i/\mathcal{V}_i$ is the entropy density. The pressure P_i and the temperature T_i are given through the equilibrium equations of state as functions of the intensive variables ρ_i, s_i. We have also introduced geometric quantities arising from the Voronoi construction: A_{ij} is the area (length in 2D) of the face between cells i, j, $\boldsymbol{e}_{ij} = (\boldsymbol{R}_i - \boldsymbol{R}_j)/R_{ij}$ with $R_{ij} = |\boldsymbol{R}_i - \boldsymbol{R}_j|$ being the unit vector normal to the face i, j and, finally, $\boldsymbol{c}_{ij}$ is a vector parallel to the face i, j pointing from $(\boldsymbol{R}_i + \boldsymbol{R}_j)/2$ to the centre of the face i, j.

The following term in the momentum equation in equations (1)

$$\sum_j \frac{A_{ij}}{R_{ij}}\boldsymbol{c}_{ij}\left((P_i - P_j) - \frac{\rho_i + \rho_j}{2}(\mu_i - \mu_j) - \frac{s_i + s_j}{2}(T_i - T_j)\right) \qquad (2)$$

is strongly reminiscent of the Gibbs–Duhem relation which, in differential form, is $\mathrm{d}P - \rho\mathrm{d}\mu - s\mathrm{d}T = 0$. For this reason, we expect that this term (2), although not exactly zero, is very small, and this has been checked in actual simulations [6]. It is rather easy to show that total mass $\sum_i M_i$, momentum $\sum_i \boldsymbol{P}_i$, and energy $\sum_i \boldsymbol{P}^2/2M_i + \mathcal{E}(M_i, S_i, \mathcal{V}_i)$ are conserved *exactly* and that the total entropy $\sum_i S_i$ does not change in time due to this reversible motion. It

can also be shown that the above equations can be understood as a finite volume discretization of the Euler equations for an inviscid fluid [6].

On the other hand, the reversible part of the dynamics in [5] is given in terms of energy instead of entropy. The equations for the position and mass evolution are identical to those in (1), the equation for the momentum evolution differs only in the absence of the Gibbs–Duhem term (2) and the equation for the internal energy evolution is given by [5]

$$\dot{E}_i = \sum_j \frac{A_{ij}}{R_{ij}} \frac{\epsilon_i + \epsilon_j}{2} \boldsymbol{c}_{ij} \cdot \boldsymbol{v}_{ij} - \sum_j A_{ij} \frac{p_i + p_j}{2} \boldsymbol{e}_{ij} \cdot \boldsymbol{v}_{ij} \tag{3}$$

where $\epsilon_i = E_i/\mathcal{V}_i$. It can be shown that if one computes the time derivative of the total entropy with the equations in [5], one obtains a nonzero production of entropy which involves a discrete version of the Gibbs–Duhem relation, analogous to (2). This term is expected to be very small and in practical situations is completely negligible when compared with the entropy production due to the irreversible part of the dynamics. Nevertheless, we propose an energy evolution which respects the zero entropy production of the reversible part of the dynamics. From equations (1) and the chain rule applied to $E(M_i, S_i, \mathcal{V}_i)$ one readily arrives at

$$\begin{aligned} \dot{E}_i = -\frac{\partial E_i}{\partial \mathcal{V}_i}\dot{\mathcal{V}}_i + \frac{\partial E_i}{\partial M_i}\dot{M}_i + \frac{\partial E_i}{\partial S_i}\dot{S}_i = {} & P_i \sum_j \frac{1}{2} A_{ij} \boldsymbol{e}_{ij} \cdot \boldsymbol{v}_{ij} - P_i \sum \frac{A_{ij}}{R_{ij}} \boldsymbol{c}_{ij} \cdot \boldsymbol{v}_{ij} \\ & + \mu_i \sum \frac{\rho_i + \rho_j}{2} \frac{A_{ij}}{R_{ij}} \boldsymbol{c}_{ij} \cdot \boldsymbol{v}_{ij} + T_i \sum \frac{s_i + s_j}{2} \frac{A_{ij}}{R_{ij}} \boldsymbol{c}_{ij} \cdot \boldsymbol{v}_{ij} \end{aligned} \tag{4}$$

where we have used the particular form of the volume in terms of the positions of the Voronoi cells as given in [6] and the usual thermodynamic definition of the intensive parameters P_i, T_i and μ_i. Here, the entropy $S_i = S(M_i, E_i, \mathcal{V}_i)$ should be understood as the dependent variable. It is possible to show, following the steps of [6], that equation (4) can be interpreted as a finite volume discretization, valid to first order in spatial gradients, of the continuum equation

$$\partial_t \epsilon = -\nabla \cdot (\epsilon \boldsymbol{v}) - P \nabla \cdot \boldsymbol{v}. \tag{5}$$

2.2. Irreversible part

The dissipative part in the Navier–Stokes equations involves the (negative) divergences of the stress tensor and heat flux, given by the usual forms

$$\boldsymbol{\Pi} = \eta(\nabla \boldsymbol{v} + (\nabla \boldsymbol{v})^T) \qquad \boldsymbol{J}^q = \kappa \nabla T \tag{6}$$

where η is the shear viscosity (we have assumed a zero bulk viscosity for simplicity), κ is the thermal conductivity and $(\nabla \boldsymbol{v})^T$ is the transpose of the velocity gradient tensor.

The main difference in the dissipative part of the equations between the models in [5] and [6] appears in the form selected by the discrete versions of the stress tensor and the heat flux. The comparison can be made explicit by noting that the divergence of a flux $\boldsymbol{J}$ in a given cell can be approximated, up to first order in spatial derivatives, through [6]

$$[\nabla \cdot \boldsymbol{J}]_i = -\frac{1}{\mathcal{V}_i} \sum_j A_{ij} \boldsymbol{e}_{ij} \cdot [\boldsymbol{J}]_{ij} \tag{7}$$

where $[\nabla \cdot \boldsymbol{J}]_i$ is the spatial average of $\nabla \cdot \boldsymbol{J}$ over the volume of cell i and $[\boldsymbol{J}]_{ij}$ is the spatial average of the field $\boldsymbol{J}$ over the face joining cells i, j. The physical meaning of (7) is apparent when one thinks of $A_{ij}\boldsymbol{e}_{ij}$ as the surface normal vector of face i, j.

In [5], the averages of the stress tensor and heat flux fields over the face i,j are approximated by the expressions

$$\begin{aligned}[\boldsymbol{\Pi}]_{ij}^{\alpha\beta} &= \eta\frac{1}{R_{ij}}\left(\boldsymbol{v}_{ij}^{\alpha}\boldsymbol{e}_{ij}^{\beta}+\boldsymbol{e}_{ij}^{\alpha}\boldsymbol{v}_{ij}^{\beta}\right)\\ [\boldsymbol{J}^{q}]_{ij} &= \kappa\frac{1}{R_{ij}}(T_i-T_j).\end{aligned} \tag{8}$$

On the other hand, in [6] the average $[\boldsymbol{J}]_{ij}$ of the flux over the face i, j in equation (7) is approximated by the arithmetic mean $[\boldsymbol{J}]_{ij}=([\boldsymbol{J}]_i+[\boldsymbol{J}]_j)/2$ and then, the flux $[\boldsymbol{J}]_i$ on cell i (similarly for cell j), which is given in terms of the spatial derivatives (6), is approximated again by (7). The resulting discrete stress tensor and heat flux of [6] are given by

$$\begin{aligned}[\boldsymbol{\Pi}]_{i}^{\alpha\beta} &= \frac{\eta}{\mathcal{V}_i}\left[\frac{1}{2}\sum_j A_{ij}\left[\boldsymbol{e}_{ij}^{\alpha}\boldsymbol{v}_j^{\beta}+\boldsymbol{e}_{ij}^{\beta}\boldsymbol{v}_j^{\alpha}\right]-\frac{1}{D}\delta^{\alpha\beta}\sum_j A_{ij}\boldsymbol{e}_{ij}\cdot\boldsymbol{v}_j\right]\\ [\boldsymbol{J}^{q}]_i &= \frac{\kappa}{2\mathcal{V}_i}\sum_j A_{ij}\boldsymbol{e}_{ij}T_j.\end{aligned} \tag{9}$$

The different structures of the discrete stress tensor and heat flux in equations (8) and (9) lead to different dissipative terms in the equations of motion. In the model in [5], the dissipative interactions appear in the form of pairwise interactions between the Voronoi cells, much in the spirit of the original DPD model [7, 10], whereas in the model in [6], the interaction is not pairwise, but includes information about neighbours of a given pair. This seems to have significant implications in the numerical simulations. For example, we have shown in [6] that the measured kinematic viscosity is in very good agreement with the input viscosity when the stress tensor is given by (9), while it is 10% off for the form (8) [5]. This may be due to the fact that equations (8) are too crude an approximation for the stress tensor since we actually compute the gradient only in the direction along $\boldsymbol{R}_{ij}$. In the discrete implementation in equation (9) we capture more information about the stress tensor, so producing more satisfactory numerical results.

3. Equilibrium distributions for the stochastic model

In section 2 we have discussed the deterministic equations for the discrete model of a Newtonian fluid. If the Voronoi cells are mesoscopic in their physical size, they will be subject to thermodynamic fluctuations. These fluctuations can be easily introduced following the methods of [5, 6] and we show in the appendix how they can be formulated for the model in [5] by the use of the GENERIC formalism as developed in [6]. The resulting stochastic differential equations are mathematically equivalent to a Fokker–Planck equation that governs the probability distribution function $\rho=\rho(x,t)$ that each Voronoi cell has a particular realization of the state variables denoted globally by x. In the GENERIC notation, this Fokker–Planck equation has the form [8]

$$\partial_t\rho=-\frac{\partial}{\partial x}\left[\rho\left[L\frac{\partial E}{\partial x}+M\frac{\partial S}{\partial x}\right]-k_B M\frac{\partial\rho}{\partial x}\right] \tag{10}$$

where k_B is Boltzmann's constant and L and M are the reversible and irreversible matrices, respectively.

The distribution function of the variables of a given system at equilibrium is given by the Einstein distribution function. This assertion can be proved under quite general assumptions on the mixing character of the microscopic dynamics of the system [11]. If the microscopic

dynamics ensures the existence of dynamical invariants such as the energy $E(x)$ and, perhaps, other invariants $I(x)$, then the Einstein distribution function takes the form [11]

$$\rho^{\mathrm{eq}}(x) = g(E(x), I(x)) \exp\{S(x)/k_B\} \tag{11}$$

where the function g is completely determined by the arbitrary initial distribution of the dynamical invariants. For example, if at an initial time the values of the invariants $E(x)$, $I(x)$ are known with high precision to be E_0, I_0, then the Einstein distribution function takes the form

$$\rho^{\mathrm{eq}}(x) = \frac{\delta(E(x) - E_0)\delta(I(x) - I_0)}{\Omega(E_0, I_0)} \exp\left\{k_B^{-1} S(x)\right\} \tag{12}$$

where $\Omega(E_0, I_0)$ is the normalization factor. Given the general argument behind the Einstein distribution function [11], it is sensible to demand that the Fokker–Planck equation (10) has as its (unique) equilibrium distribution function the Einstein distribution. This can be achieved if the following further conditions on the form of the matrices L, M hold [8]

$$\frac{\partial}{\partial x}\left[L\frac{\partial E}{\partial x}\right] = 0 \qquad M\frac{\partial I}{\partial x} = 0. \tag{13}$$

The second condition is just the requirement that the dissipative part of the dynamics should conserve the total mass, energy and momentum of the system. The first condition can be understood as an incompressibility condition on the reversible dynamics of the system in the state space x. We should note that this incompressibility equation is only approximately satisfied by our reversible dynamics. Nevertheless, as we will show in what follows, the Einstein distribution function is still a very good approximation for the equilibrium solution of the Fokker–Planck equation.

3.1. Equilibrium N-particle distribution function

In this section we discuss the equilibrium distribution function $\rho^{\mathrm{eq}}(x)$ corresponding to the equations of motion of our discrete models [5, 6]. Note that the equilibrium distribution function is the same, irrespective of the actual form of the irreversible part of the dynamics. This is because both sets of equations have the so-called GENERIC structure. The GENERIC structure of the equations of motion ensures that the equilibrium distribution function for these variables is given by the Einstein distribution function in the presence of dynamical invariants (equation (11)). As the total mass $M(x)$, total energy $E(x)$ and momentum $\boldsymbol{P}(x)$ are conserved by the dynamics, the Einstein distribution function will be given in our models by

$$\rho^{\mathrm{eq}}(x) = \frac{1}{\Omega}\delta(M(x) - \mathcal{M}_0)\delta(E(x) - E_0)\delta(\boldsymbol{P}(x) - \boldsymbol{P}_0) \times \exp\left\{k_B^{-1} S(x)\right\} \tag{14}$$

where we have assumed that we know with absolute precision the values of the total mass $\mathcal{M}_0$, energy E_0 and momentum $\boldsymbol{P}_0$ at the initial time. This is the situation in a computer simulation. Here Ω is a factor that ensures the correct normalization of $\rho^{\mathrm{eq}}(x)$. The total energy and entropy in our models have the forms $E(x) = \sum_i P_i^2/2M_i + E_i$ and $S(x) = \sum_i S_i$.

A word is in order about the total volume. We note that *any* configuration of positions $\boldsymbol{R}_i$ of the Voronoi particles has the property that the total volume is conserved $\sum_i \mathcal{V}_i = \mathcal{V}_0$. Therefore, even though the total volume is conserved, it does not produce a restriction in the form of a delta function in equation (14). Actually, for our models, it is more convenient to consider the probability of a particular realization of the total set of variables $\{V, \boldsymbol{P}, M, S\}$ instead of $\{\boldsymbol{R}, \boldsymbol{P}, M, S\}$. This is calculated as

$$P(\{V, \boldsymbol{P}, M, S\}) = \int \{\mathrm{d}\boldsymbol{R}\}\delta^N(V - \mathcal{V}(\{\boldsymbol{R}\}))\rho^{\mathrm{eq}}(x). \tag{15}$$

Because $\rho^{\mathrm{eq}}(x)$ depends on the positions only through the volume variable, we have

$$P(\{V, \boldsymbol{P}, M, S\}) = F(V_1, \ldots, V_N)\rho^{\mathrm{eq}}(\{V, \boldsymbol{P}, M, S\}) \tag{16}$$

where

$$F(V_1, \ldots, V_N) = \int \mathrm{d}\{\boldsymbol{R}\} \prod_i^N \delta(V_i - \mathcal{V}_i(\{\boldsymbol{R}\})). \tag{17}$$

This function F is proportional to the probability density that the particles have the particular distribution of volumes $V_1, \ldots, V_N$ provided that the distribution function of the positions is uniform. Note that, because $F(V_1, \ldots, V_N)$ does not contain information about the location of the volumes, we expect that the probability that a given cell has a particular volume is independent of the vast majority of the volumes of the rest of the cells. In this way, we expect that an approximation in which the volumes are statistically independent in a random distribution of cells might be a good one, particularly if the number M of cells is very large. However, there is a global correlation that must be respected, namely that of total volume conservation. Therefore, we expect

$$F(V_1, \ldots, V_N) \propto F(V_1) \cdots F(V_N)\delta\left(\sum_i V_i - \mathcal{V}_0\right) \tag{18}$$

where $F(V)$ is the probability density that, in a random distribution of points, the volume of a Voronoi cell is V, irrespective of the values of the volumes of other cells. The exact analytical calculation of the function $F(V)$ is difficult, but a phenomenological expression has been given in [12]. As the only scale in a random distribution of points is the average volume of each cell, the volume distribution function should have a scaling form

$$F(V) = \frac{1}{\bar{V}}\phi\left(\frac{V}{\bar{V}}\right) \tag{19}$$

where $\bar{V}$ represents the mean volume value for the cell. The function $\phi(x)$ is the gamma distribution function [12]

$$\phi(x) = \frac{\nu^\nu}{\Gamma(\nu)} x^{\nu-1} \exp\{-\nu x\} \tag{20}$$

properly normalized to unity, $\int_0^\infty \phi(x)\,\mathrm{d}x = 1$. Here, ν is a constant parameter governing the shape of the distribution.

In figure 1 we plot the cell volume distribution of a Voronoi tessellation of an ensemble of uniform random sets of points, together with a fitted gamma distribution with value $\nu = 3.8420$ and $\bar{V} = 0.0025$.

3.2. The most probable state

The most probable state at equilibrium according to equation (14) is the one that maximizes the entropy $S(x)$ subject to the constraints $M(x) = M_0$, $E(x) = E_0$ and $\boldsymbol{P}(x) = \boldsymbol{P}_0$. By introducing Lagrange multipliers β, λ and $\boldsymbol{V}$, the most probable state is the one that maximizes $k_B^{-1}S(x) - \beta(E(x) - \boldsymbol{V}\cdot\boldsymbol{P}(x) - \lambda M(x))$ without constraints. By equating the partial derivatives with respect to every variable to zero, one obtains the following implicit equations for the most probable values $x^* = \{\boldsymbol{R}_i^*, \boldsymbol{P}_i^*, M_i^*, S_i^*\}$ where * indicates the most probable state

$$\sum_j \frac{\partial \mathcal{V}_j}{\partial \boldsymbol{R}_i} P_j(x^*) = 0 \qquad \frac{\boldsymbol{P}_i^*}{M_i^*} = \boldsymbol{V} \qquad \mu_i(x^*) = \lambda + \frac{D}{2}\boldsymbol{V}^2 \qquad T_i(x^*) = \frac{1}{k_B\beta} \tag{21}$$

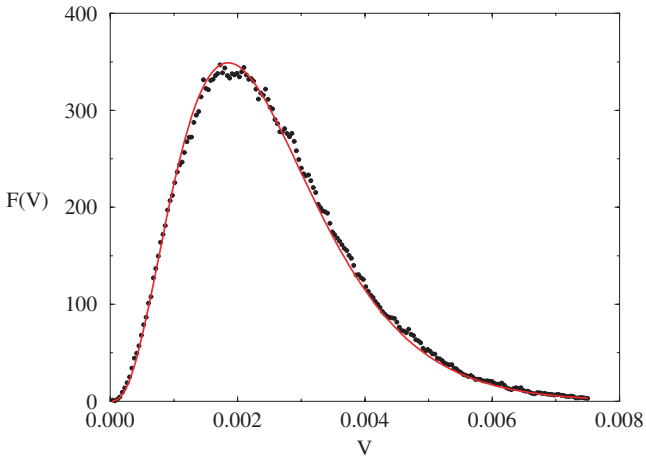

Figure 1. Distribution function for the Voronoi volume of a random distribution of points for a simulation with $M = 400$ particles in a two-dimensional periodic boundary box of length $L = 1$ (dots). The continuous line corresponds to equation (19) with $\nu = 3.8420$ and $\bar{V} = 0.0025$.

where D is the number of space dimensions. The second equation in (21) states that in the most probable state all particles move at the same velocity $\boldsymbol{V}$ which might be set to zero without loss of generality. The last two equations state, then, that the chemical potential per unit mass and the temperature of all the fluid particles are equal at the most probable value of the discrete hydrodynamic variables. This implies that the pressure is also the same for all the fluid particles (in a simple fluid the intensive parameters are not independent [13]). The first equation is, therefore, trivially satisfied (because $\sum_j \mathcal{V}_j = \mathcal{V}_0$, which is independent of $\boldsymbol{R}_i$).

3.3. Equilibrium single-particle distribution function

In order to compare simulation and theoretical results, it is necessary to consider the single-particle distribution function instead of the multidimensional N-particle distribution. For this reason, as a first step, we will integrate all the momentum variables except that of the first particle. The outcome will be to convert the 'microcanonical' distribution (14) into a 'canonical' distribution. Afterwards, we will integrate over the volume, mass and entropy of all the particles except the first particle. We denote the state by $x = (y, \{\boldsymbol{P}\})$ where $y = (\{V\}, \{M\}, \{S\})$ is the set of volumes, masses and entropies of all particles. Note that the total entropy and internal energy do not depend on momentum variables.

By integrating the distribution function $\rho^{\mathrm{eq}}(x)$ over all momenta except $\boldsymbol{P}_1$ we obtain the probability $\rho^{\mathrm{eq}}(\boldsymbol{P}_1, y)$

$$\rho^{\mathrm{eq}}(\boldsymbol{P}_1, y) = \prod_i \frac{F(V_i)}{\Omega_0} \exp\left\{\frac{S(y)}{k_B}\right\} \delta\left(\sum_i^N M_i - \mathcal{M}_0\right) \delta\left(\sum_i^N V_i - \mathcal{V}_0\right) \times \prod_{\mu=2}^N (2M_i)^{D/2} \frac{\omega_{D(N-2)}}{2} \left[E_0 - \sum_i E_i(y) - \frac{\boldsymbol{P}_1^2}{2M_1}\right]^{\frac{D(N-2)}{2}-1} \tag{22}$$

where we have used the following equation, which is proved in appendix VII of [14],

$$\int \mathrm{d}^{DN}\boldsymbol{P}\, \delta\left(\sum_i^N \frac{\boldsymbol{P}_i^2}{2M_i} - E_0\right) \delta^D\left(\sum_i^N \boldsymbol{P}_i - \boldsymbol{P}_0\right) = \frac{1}{2}\omega_{D(N-1)} U_0^{\frac{D(N-1)-2}{2}} \prod_i^N (2M_i)^{D/2} \tag{23}$$

where D is the spatial dimensionality, $U_0 = E_0 - P^2{}_0/2M_0$, and

$$\omega_N = 2\frac{\pi^{N/2}}{\Gamma(N/2)}. \tag{24}$$

We now find a convenient approximation to equation (22) by noting that this probability is expected to be highly peaked around the most probable state. Therefore, for those values of $\mathcal{E}_i(y)$ for which $\rho^{\mathrm{eq}}(\boldsymbol{P}_1, y)$ is appreciably different from zero we can approximate it with an exponential

$$\left[E_0 - \sum_i E_i - \frac{\boldsymbol{P}_1^2}{2M_1}\right]^P \propto \exp\left\{-\beta^*\left(\sum_i E_i + \frac{\boldsymbol{P}_1^2}{2M_1}\right)\right\} \tag{25}$$

where $P = D(M-2)/2 - 1 \gg 1$. We have introduced the parameter β^* as

$$\beta^* = \frac{D(M-1)/2 - 1}{E_0 - \sum_j E_j^*} \approx \frac{DM/2}{E_0 - \sum_j E_j^*} \tag{26}$$

where $E_i{}^*$ is the most probable value of E_i. The parameter β^* is proportional to the inverse of the most probable kinetic energy. Finally, we can write equation (22) as

$$\rho^{\mathrm{eq}}(\boldsymbol{P}_1, y) = \prod_i \frac{F(V_i)}{\Omega_0}\delta\left(\sum_i^N M_i - \mathcal{M}_0\right)\delta\left(\sum_i^N V_i - \mathcal{V}_0\right) \times \exp\left\{\frac{S(y)}{k_B} - \beta^*\sum_i^N E_i(y) - \beta^*\frac{\boldsymbol{P}_1^2}{2M_1}\right\} \tag{27}$$

where Ω_0 is a normalization constant. In equation (27) we have neglected a term $\sum_i \log M_i$ since it is much less than $\sum_i E_i(y)$. Note that $\mathcal{E}_i$ is a first-order function of its arguments S_i, M_i, V_i and, therefore, it is of order M_i.

We are also interested in the distribution function $P(V_1, \boldsymbol{P}_1, M_1, S_1)$. This is the probability that a particular mesoparticle takes the values $V_1, \boldsymbol{P}_1, M_1, S_1$ for its variables, independently from the values of the rest of the variables in the system. We want to integrate (27) over the variables V, M, S of all particles except $V_1, \boldsymbol{P}_1, M_1, S_1$. We can rewrite

$$P(V_1, \boldsymbol{P}_1, M_1, S_1) = \frac{1}{\Omega_0'}F(V_1)\Phi(\mathcal{M}_0 - M_1, \mathcal{V}_0 - V_1) \times \exp\left\{\frac{S_1}{k_B} - \beta^* E_1(M_1, S_1, V_1) - \beta^*\frac{\boldsymbol{P}_1^2}{2M_1}\right\} \tag{28}$$

where we have introduced the function

$$\Phi(\mathcal{M}, \mathcal{V}) = \int \mathrm{d}^{(N-1)}\{V\}\mathrm{d}^{(N-1)}\{M\}\mathrm{d}^{(N-1)}\{S\}\prod_{i=2}^N F(V_i)\delta\left(\sum_{i=2}^N M_i - \mathcal{M}\right) \times \delta\left(\sum_{i=2}^N V_i - \mathcal{V}\right)\exp\left\{\sum_{i=2}^N \frac{S_i}{k_B} - \beta^* E_i(M_i, S_i, V_i)\right\}. \tag{29}$$

The functional form of $\Phi(\mathcal{M}, \mathcal{V})$ is very well approximated by an exponential, as can be seen by taking derivatives with respect to $\mathcal{M}$ and $\mathcal{V}$. We expect that when the number of variables M is very large, the integrand becomes highly peaked around this most probable value and then direct computations show

$$\frac{\partial}{\partial \mathcal{M}}\Phi(\mathcal{M}, \mathcal{V}) \approx -\beta^*\lambda^*\Phi(\mathcal{M}, \mathcal{V}) \qquad \frac{\partial}{\partial \mathcal{V}}\Phi(\mathcal{M}, \mathcal{V}) \approx \beta^*\Pi^*\Phi(\mathcal{M}, \mathcal{V}) \tag{30}$$

where Π^* and λ^* are suitable Lagrange multipliers accounting for the mass and volume conservation. Therefore,

$$\Phi(\mathcal{M}, \mathcal{V}) \approx \exp\{-\beta^*(\lambda^*\mathcal{M} - \Pi^*\mathcal{V})\}. \tag{31}$$

Returning to equation (28) we have the final result for the single-particle distribution function as

$$P(V_1, \boldsymbol{P}_1, M_1, S_1) = \frac{1}{Z}F(V_1)\exp\left\{\frac{S_1}{k_B} - \beta^*\left(E(M_1, S_1, V_1) + \frac{\boldsymbol{P}_1^2}{2M_1} - \lambda^* M_1 + \Pi^* V_1\right)\right\} \tag{32}$$

where Z is an appropriate normalization factor. The form of the single-particle distribution function can be interpreted as the probability that a subsystem that can exchange mass, momentum, energy and volume with a thermal bath (whose intensive parameters are β^*, λ^*, Π^*) has particular values of these extensive variables. Note that, although the momentum distribution looks Gaussian, it is not statistically independent of the mass. Regarding the volume, the presence of the factor $F(V)$ inhibits an interpretation of Π^* as giving directly the pressure of the thermal bath.

The most probable values of the single-particle distribution function (32), denoted with a double star, are given by

$$P_i^{**} + \frac{F'(V)}{\beta^* F(V)} = \Pi^* \qquad \boldsymbol{P}_i^{**} = \boldsymbol{0} \qquad \mu_i^{**} = \lambda^* \qquad T_i^{**} = \frac{1}{k_B\beta^*} \tag{33}$$

which should be compared with equations (21). Here, P_i^{**} is the most probable value of the pressure of particle i. Note the connection between β^* (related to the most probable value of the kinetic energy) and the most probable thermodynamic temperature in equation (33). Note also that the most probable value of the single-particle distribution function x^{**} in equation (33) does not exactly coincide with the most probable value of the N-particle distribution function x^* of equations (21) due to the integrations involved. However, the discrepancies are expected to be very small.

3.4. Single-variable distribution functions of a mesoparticle

Note that, in a simulation, it is difficult to measure the distribution function (32) due to the large number of variables involved (five), which would necessitate binning of frequencies of occurences in a five-dimensional space. Clearly what we need are the distribution functions over a single variable. In this section, we compute these further marginal distribution functions.

The joint probability distribution function of the volume, mass and entropy of one particle is easily obtained because the momentum variables $\tilde{\boldsymbol{P}}$ are trivially integrated

$$P(V, M, S) \propto \frac{1}{Z}F(V)\left(\frac{2\pi M}{\beta^*}\right)^{\frac{D}{2}}\exp\left\{\frac{S}{k_B} - \beta^*(E(M, S, V) - \lambda^* M + \Pi^* V)\right\}. \tag{34}$$

By making use of the analytical expression for $F(V)$ in equation (19), and performing a change of variables from entropy S to internal energy E, for an ideal gas, we can calculate the mass and volume distribution function. The Jacobian is given by the temperature $T(E)$. The integral can be performed analytically and the result is (from now on we assume $D = 2$)

$$P(V, M) \propto (V)^{\nu-1}M^2\left(\frac{cVe^2}{M^2\beta^*}\right)^{\frac{M}{m_0}}\Gamma\left(\frac{M}{m_0}\right)\exp\left\{-\nu\frac{V}{\bar{V}} + \beta^*(\lambda^* M - \Pi^* V)\right\} \tag{35}$$

where $\Gamma(x)$ is the gamma function, $e = \exp(1)$, m_0 is the mass of the molecule of ideal gas we are simulating and c is a dimensionless constant that depends only on microscopic

parameters, being defined as the ratio between λ the typical distance between molecules at chosen temperature T_e and Λ the thermal wavelength

$$c = \left(\frac{\lambda}{\Lambda}\right)^2 = \frac{\lambda^2 2\pi m_0 k_B T_e}{h^2}. \tag{36}$$

We can now integrate over the volume variable in $P(V, M)$ to obtain the mass distribution function. Note that the integration limits are extended to $(0, \infty)$ because the range of variation for one particle's mass is very small compared to the total mass of the system,

$$P(M) \propto \int_0^\infty P(V, M)\,\mathrm{d}V \propto \Gamma\left(\frac{M}{m_0}\right)\Gamma\left(\nu + \frac{M}{m_0}\right)\left(\frac{M}{m_0}\right)^{2\left(1-\frac{M}{m_0}\right)} \times \left(\frac{ce^2}{k_B^2\beta^*\left(\beta^*\Pi^* + \frac{\nu}{\bar{V}}\right)}\right)^{\frac{M}{m_0}} \exp\{\beta^*\lambda^* M\}. \tag{37}$$

We next calculate the volume distribution function by integrating over the mass in equation (35) as

$$P(V) \propto (V)^{\nu-1} \exp\left\{-\nu\frac{V}{\bar{V}} - \beta^*\Pi^* V\right\} g(V, \beta^*, \lambda^*) \tag{38}$$

where the function $g(V, \beta^*, \lambda^*)$ is defined as

$$g(V, \beta^*, \lambda^*) = \int_0^\infty M^{2\left(1-\frac{M}{m_0}\right)}\left(\frac{cVe^2}{\beta^*}\right)^{\frac{M}{m_0}}\Gamma\left(\frac{M}{m_0}\right)\exp\{\beta^*\lambda^* M\}\mathrm{d}M. \tag{39}$$

We can extract the density distribution function very easily from equation (35)

$$P(\rho) = \int P(V, M)\delta\left(\rho - \frac{M}{V}\right)\mathrm{d}V\,\mathrm{d}M = \int P(V, \rho V)V\,\mathrm{d}V \propto \rho^2 h(\rho, \lambda^*, \beta^*, \Pi^*) \tag{40}$$

where we have introduced the function

$$h(\rho, \lambda^*, \beta^*, \Pi^*) = \int_0^\infty V^{\nu+2}\left(\frac{cVe^2}{(\rho V)^2\beta^*}\right)^{\frac{\rho V}{m_0}}\Gamma\left(\frac{\rho V}{m_0}\right) \times \exp\left\{\left(-\frac{\nu}{\bar{V}} + \beta^*(\lambda^*\rho - \Pi^*)\right)V\right\}\mathrm{d}V. \tag{41}$$

Finally, we consider the momentum distribution function. After carrying out the entropy and volume integrations in equation (32) we obtain

$$P(P^x) = \sqrt{\frac{\beta^*}{2\pi}}\int\frac{P(M)}{\sqrt{M}}\exp\left\{-\beta^*\frac{P^{x2}}{2M}\right\}\mathrm{d}M. \tag{42}$$

4. Simulation results

We have already mentioned that the dissipative terms in the model of [6] produce slightly better numerical results than those of [5] and for this reason we present the simulation data for this model. The specific details of the simulations are those in [6]. We simulate $N_{mic} =$ 40 000 atoms of argon, assumed to be an ideal gas. The system is at temperature $T_e = 273$ K in a periodic boundary box. The typical distance between molecules in an ideal gas at room temperature and pressure in three dimensions is about $\lambda = 3 \times 10^{-9}$ m. If in two dimensions we want to keep this typical distance, then the linear dimensions of our simulation box should be $L = N_{mic}^{\frac{1}{2}}\ 3 \times 10^{-9}$ m $= 6.67 \times 10^{-7}$ m. In the following, all quantities are expressed in

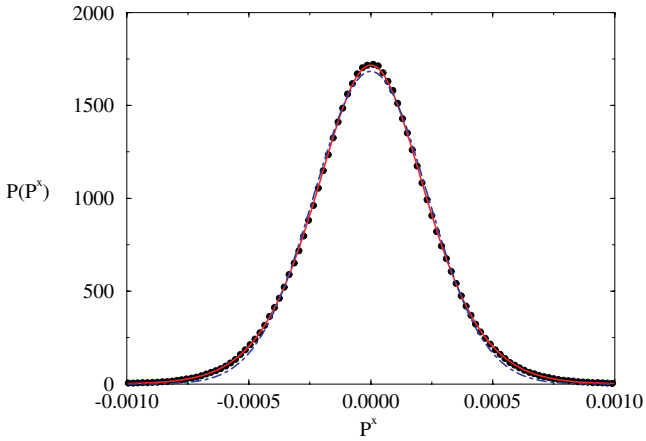

Figure 2. Equilibrium momentum distribution function. The dotted line corresponds to the simulation results for $P(P^x)$. The continuous line corresponds to our prediction in equation (42) for the value of $\beta^* = 39\,947.26$. The broken line corresponds to the best Gaussian fit; note, however, that this should correspond to a system with a fixed mass of particles, which is not actually the case in our simulations, as can be seen from the mass distribution function shown in figure 4.

the reduced units defined in [6]. These simulations are performed using $M = 400$ mesoscopic particles in a 2D box with box length $L = 1$, with constant shear and bulk viscosities and thermal conductivity such that $\eta = \zeta = \kappa = 0.01$. These mesoscopic particles contain typically 100 argon atoms. In reduced units the temperature is initially set to $T = 1$ and the density to $\rho = 1$.

The stochastic equations are integrated with an Euler scheme that conserves total momentum and energy with a time step $\mathrm{d}t = 0.000\,001$ in reduced units. The initial state is set as follows. From a random distribution of dissipative particle positions in the box, we obtain the Voronoi volumes. We initialize the mesoparticle masses in such a way that we obtain a constant density for the particles, equal to the global density of the system ($\rho = 1$). Then the initial entropies and temperatures are calculated using the corresponding functions for the ideal gas. The initial velocities are set to zero and consequently the total momentum is zero. Note that this initial state, although close to equilibrium, is not an equilibrium state. We let the system evolve to the equilibrium state and measure the equilibrium momentum, mass and volume distribution functions.

The equilibrium momentum distribution function measured in the simulations is plotted in figure 2. As a first approximation, we can fit it to a Gaussian function (broken line). It is a reasonable fit, but we observe some significant discrepancies. The origin arises from the fact that momentum and mass are not statistically independent. Of course, the momentum distribution function is actually given by equation (42). If we use this equation with the distribution function for the mass obtained in the simulations we obtain better agreement. The best fit for the parameter is $\beta^* = 39\,947.26$, in perfect agreement with the value $\beta^* = \frac{1}{k_b T_e}$ provided by the global temperature of the ideal gas system compatible with the total mass, momentum and energy of the system.

The identity between the kinetic temperature (given through β^*) and the thermodynamic temperature in equation (33) is validated in the results shown in figure 3, where we plot the

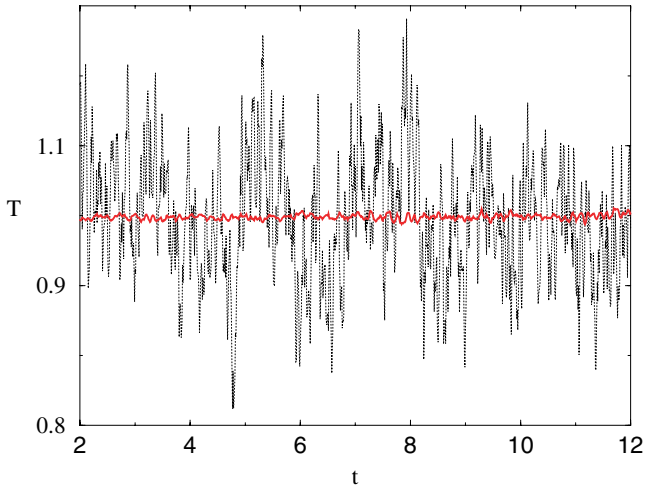

Figure 3. Time evolution for the kinetic and thermodynamic temperatures (dotted and continuous lines, respectively). The mean values are $T_{\text{thermo}} = 1.000 \pm 0.004$ and $T_{\text{kin}} = 1.00 \pm 0.08$, in reduced units. The kinetic temperature has bigger fluctuations, associated with the width of the momentum distribution function in figure 2.

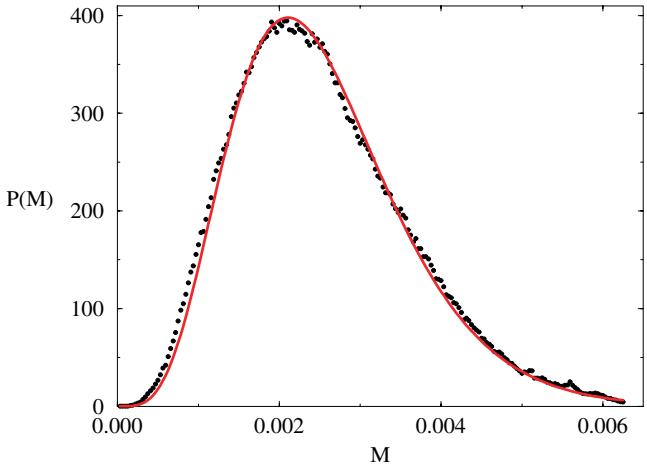

Figure 4. Mass equilibrium distribution function. Dots correspond to simulation results. The continuous line is the fit to equation (37) for the parameters $\beta^* = 39\,947.26$, $\Pi^* = 1.009\,604$ and $\lambda^* = -10.619\,795$.

average kinetic energy per mesoparticle and the mean of all thermodynamic temperatures obtained from the equation of state for each mesoparticle.

In figures 4–6 we show the mass, volume and density equilibrium distribution functions for a single mesoparticle. Solid lines show the best fits of the simulation results to the nonlinear functions dependent on the three parameters (β^*, Π^*, λ^*) given in equations (37), (38) and (40). These fits have been obtained through a standard Levenberg–Marquardt nonlinear least-squares routine. The parameter β^* has been fitted from the momentum distribution function. It is interesting to note that many pairs of values for Π^*, λ^* provide individually reasonable fits for the simulation data $P(M)$, $P(V)$, $P(\rho)$. For this reason, we have minimized

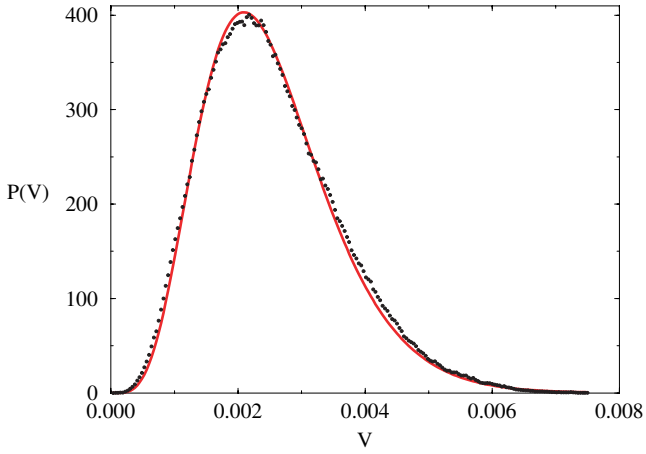

Figure 5. Volume equilibrium distribution function. Dots correspond to simulation results. The continuous line is the fit to equation (38) for the fitted values $\beta^* = 39\,947.26$, $\Pi^* = 1.009\,604$ and $\lambda^* = -10.619\,795$.

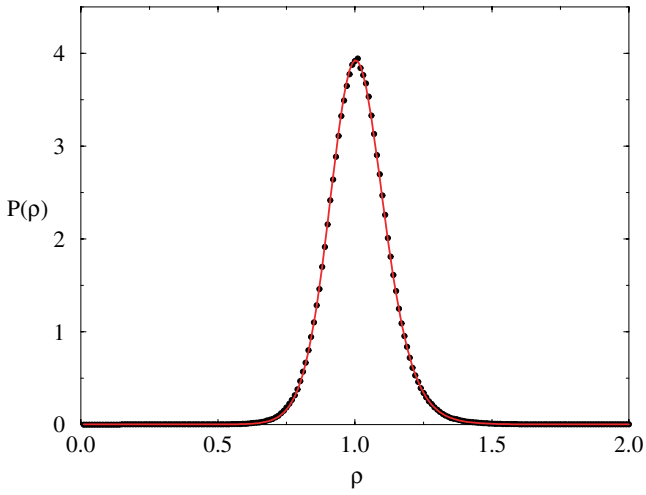

Figure 6. Density equilibrium distribution function. Dots correspond to simulation results. The continuous line is the fit to equation (40) for the fitted values $\beta^* = 39\,947.26$, $\Pi^* = 1.009\,604$ and $\lambda^* = -10.619\,795$.

simultaneously the least-squares function for the three distributions. This procedure leads to the optimal values $\beta^* = 39\,947.26$, $\Pi^* = 1.009\,604$ and $\lambda^* = -10.619\,795$. According to equations (33) the Lagrange multipliers are directly connected with the most probable values of the intensive parameters in the simulation. We have measured by direct simulation the marginal equilibrium distributions of the intensive variables and find $T^{**} = 1.001\,32$, $P^{**} = 0.993\,759$ and $\lambda^{**} = -10.5556$. We obtain perfect agreement with the temperature and reasonable agreement with the pressure and chemical potential.

The size of the fluctuations, that is, the width of the distribution functions, depends on the actual typical size of the Voronoi cells. For a given value of the density, for example, the larger the volume (and the mass) of the cell, the smaller the width of the equilibrium distribution

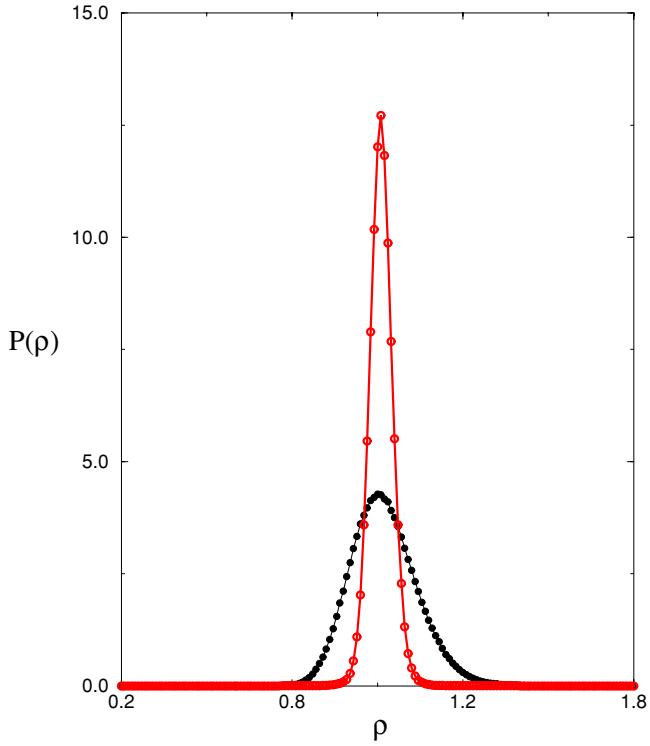

Figure 7. Density equilibrium distributions for two different typical mean mesoparticle volumes ($\bar{V} = 100$, $\bar{V} = 200$) and the same mean density $\rho = 1$. The plot with smaller width corresponds to the bigger mean volume.

function for the density, in accordance with the usual predictions of equilibrium statistical mechanics. This is illustrated in figure 7. In a general situation, the size of the cells is dictated by the relevant hydrodynamic length scale that must be resolved. Typically, the 'radius' of a cell must be 20 times smaller than the relevant hydrodynamic length scale [6], accounting for why it is necessary to include thermal fluctuations to simulate the hydrodynamic flow around a micron-sized colloidal particle but not for simulating the flow around a centimetre-sized ping pong ball.

When fluctuations are present, the entropy function $S(x)$ might sometimes be a *decreasing* function of time in a general situation. We show an example of this behaviour in figure 8 in an equilibrium situation. Of course, the fluctuations are small in macroscopic terms. However, if one considers the entropy *functional*

$$\mathcal{S}[\rho_t] = \int S(x)\rho(x,t)\,\mathrm{d}x - k_B \int \rho(x,t)\ln\rho(x,t)\,\mathrm{d}x \tag{43}$$

it is possible to prove by using the Fokker–Planck equation (10) that $\partial_t \mathcal{S}[\rho_t] \geqslant 0$ [8]. In other words, the entropy functional plays the role of a Lyapunov function. At equilibrium, the entropy $S(x)$ should be a constant (its maximum value). In a stochastic simulation, however, there are fluctuations in the entropy and, as a consequence, it might increase or decrease. Of course, if the mesoparticles are very large (in the thermodynamic limit), the fluctuations are negligible and the entropy function will be a monotonically increasing function of time.

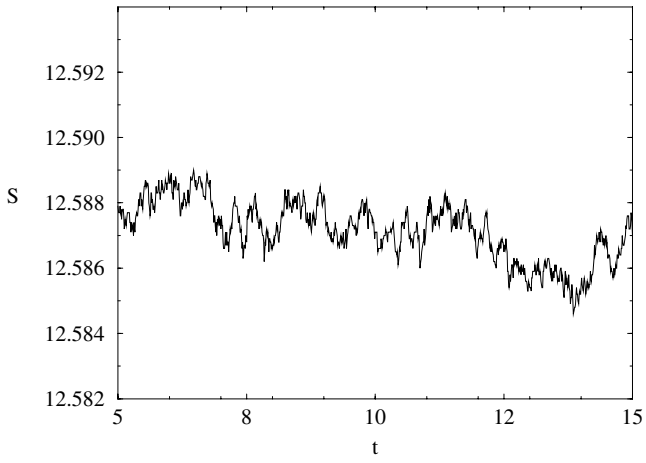

Figure 8. Time evolution for the total entropy $S(x)$ of a system with noise. Simulation details correspond to those of figures 4–6.

5. Discussion

In this paper we have discussed the relationship between two recently introduced models based on mesoscopic Voronoi fluid particles [5, 6]. From a macroscopic perspective, the models can be interpreted as finite volume discretizations of the Navier–Stokes equations in a Lagrangian description. They include thermal fluctuations that obey a fluctuation–dissipation theorem at the discrete level and, as a consequence, the equilibrium distribution function is given by the Einstein distribution function. The molecularly based model in [5] has a reversible part that produces a slight entropy increase which, strictly speaking, should be conserved. Nevertheless, in practical situations this unphysical reversible entropy production is expected to be negligible in comparison with the entropy production due to the irreversible part of the dynamics. Concerning the latter, the models differ in the discrete approximations used for the stress tensor and heat flux. It appears that the discretization in [6] produces better results for numerical values of the transport coefficients due to its non-pairwise form.

We have computed analytically the marginal distribution functions corresponding to a single mesoparticle from the Einstein distribution function, which is defined over all the variables in the system. In practice, these are the only available distributions in a simulation. Excellent agreement is obtained between the theoretical results and the simulations, conferring full confidence in the models.

Several points concerning the actual implementation of the algorithms are worth mentioning. For example, the volume distributions are broad and, this might cause spatial resolution to be different in different flow regions. One might have large fluid particles coexisting with smaller ones. However, the size of the largest fluid particles compared to the hydrodynamic length scale to be resolved is what determines the appropriate resolution for the flow problem. Because the number of largest fluid particles is given by the total number of fluid particles, it is always possible to resolve a flow with a prescribed accuracy. Regarding time integration, we have used a simple Euler scheme in order to integrate the stochastic equations. This method requires very small time steps in order to reach the desired level of energy conservation. We are currently developing higher order stochastic schemes that allow time steps two orders of magnitude larger with the same level of energy conservation, and a

three-dimensional version of the model [6], which has been recently implemented using the CGAL library [15]. We hope to report on this work in the near future.

Acknowledgments

This research has been partially supported by DGYCIT PB97-0077 (Spain) and the SIMU Project (European Science Foundation). GDF thanks Queen Mary, University of London, and Schlumberger Cambridge Research for funding his PhD studentship. PVC and GDF are grateful to CGAL for their help and support.

Appendix. 'GENERIC' structure of the irreversible part of the dynamics

In this appendix we show that the irreversible part of the dynamics of the model in [5] can be cast in the GENERIC formalism. We follow the notation in [6].

In order to derive the irreversible part of the dynamics of the DPD model and to get thermodynamically consistent thermal fluctuations, a very useful route is to first postulate the thermal noises $\mathrm{d}\tilde{x}$ and *then* construct the dissipative matrix M through the fluctuation–dissipation theorem,

$$M = \frac{\mathrm{d}\tilde{x}\,\mathrm{d}\tilde{x}^T}{2k_B\,\mathrm{d}t}. \tag{44}$$

In order to have conservation of the energy $E(x)$ and other possible dynamical $I(x)$, such as momentum, the following restrictions apply on the noises

$$\frac{\partial E}{\partial x}\,\mathrm{d}\tilde{x} = 0 \qquad \frac{\partial I}{\partial x}\,\mathrm{d}\tilde{x} = 0 \tag{45}$$

which ensure the usual GENERIC degeneracy requirements

$$M\frac{\partial E}{\partial x} = 0 \qquad M\frac{\partial I}{\partial x} = 0. \tag{46}$$

We postulate the following form for the thermal noises $\mathrm{d}\tilde{x} = \{0, \mathrm{d}\tilde{\boldsymbol{P}}_i, \mathrm{d}\tilde{E}_i\}$. Note that we do not assume any fluctuation in the mass, in accordance with the expectation that the mass equation does not contain any irreversibility. The momentum and energy random terms are postulated to be

$$\begin{aligned}\mathrm{d}\tilde{\boldsymbol{P}}_i &= \sum_j B_{ij}\,\mathrm{d}\bar{\mathbf{W}}_{ij}\boldsymbol{e}_{ij}\\ \mathrm{d}\tilde{E}_i &= -\frac{1}{2}\sum_j B_{ij}\,\mathrm{d}\bar{\mathbf{W}}_{ij}\colon\boldsymbol{e}_{ij}\cdot\boldsymbol{v}_{ij} + \sum_j C_{ij}\,\mathrm{d}V_{ij}.\end{aligned} \tag{47}$$

Here, i, j label the Voronoi cells, $\boldsymbol{e}_{ij} = \boldsymbol{R}_{ij}/|\boldsymbol{R}|_{ij}$ is the unit vector joining the cell centres, and $\boldsymbol{v}_{ij} = \boldsymbol{v}_i - \boldsymbol{v}_j$ is the relative velocity between cells i, j. The double dot means double contraction. We have introduced, for each pair i, j of (neighbour) cells, a matrix of independent increments of the Wiener process $\mathrm{d}\mathbf{W}_{ij}$. Its traceless symmetric part $\mathrm{d}\bar{\mathbf{W}}_{ij}$ is given by

$$\mathrm{d}\bar{\mathbf{W}}_{ij}^{\alpha\beta} = \tfrac{1}{2}\left[\mathrm{d}\mathbf{W}_{ij}^{\alpha\beta} + \mathrm{d}\mathbf{W}_{ij}^{\beta\alpha}\right] \tag{48}$$

where D is the space dimension. As a convention, superscripts refer to tensorial components while subscripts label different cells.

In equation (47) we have also introduced an independent increment of the Wiener process for each pair of (neighbour) cells, $\mathrm{d}V_{ij}$. Finally, the functions B_{ij}, C_{ij} might depend on the

state of the system through the mass and internal energy of the particles. We postulate the following symmetry properties

$$\mathrm{d}\mathbf{W}_{ij} = \mathrm{d}\mathbf{W}_{ji} \qquad \mathrm{d}V_{ij} = -\mathrm{d}V_{ji} \qquad B_{ij} = B_{ji} \qquad C_{ij} = C_{ji}. \tag{49}$$

The independent increments of the Wiener processes satisfy the following Itô mnemotechnical rules

$$\begin{aligned} &\mathrm{d}\mathbf{W}_{ii'}^{\alpha\alpha'}\,\mathrm{d}\mathbf{W}_{jj'}^{\beta\beta'} = [\delta_{ij}\delta_{i'j'} + \delta_{ij'}\delta_{i'j}]\delta^{\alpha\beta}\delta^{\alpha'\beta'}\,\mathrm{d}t \\ &\mathrm{d}V_{ii'}\,\mathrm{d}V_{jj'} = [\delta_{ij}\delta_{i'j'} - \delta_{ij'}\delta_{i'j}]\,\mathrm{d}t \\ &\mathrm{d}\mathbf{W}_{ii'}^{\alpha\alpha'}\,\mathrm{d}V_{jj'} = 0 \end{aligned} \tag{50}$$

which respect the symmetries (49) under particle interchange. The properties (50) imply the following stochastic properties of the noise in equation (48)

$$\mathrm{d}\mathbf{W}_{ii'}^{\alpha\alpha'}\,\mathrm{d}\mathbf{W}_{jj'}^{\beta\beta'} = \tfrac{1}{2}[\delta_{ij}\delta_{i'j'} + \delta_{ij'}\delta_{i'j}][\delta^{\alpha\beta}\delta^{\alpha'\beta'} + \delta^{\alpha\beta'}\delta^{\alpha'\beta}]\,\mathrm{d}t. \tag{51}$$

The dynamical invariants are the total linear momentum and the total energy (no angular momentum conservation is imposed). These total quantities are given by

$$E(x) = \sum_i \frac{\boldsymbol{P}_i^2}{2M_i} + E_i \qquad P(x) = \sum_i \boldsymbol{P}_i. \tag{52}$$

Their derivatives with respect to the state variables are

$$\frac{\partial E}{\partial x} \to \begin{pmatrix} -\frac{v_j^2}{2} \\ \boldsymbol{v}_j \\ 1 \end{pmatrix} \qquad \frac{\partial \boldsymbol{P}}{\partial x} \to \begin{pmatrix} 0 \\ \mathbf{1} \\ 0 \end{pmatrix} \tag{53}$$

where $\boldsymbol{v}_j = \boldsymbol{P}_j/M_j$ is the velocity of cell i. It is a trivial exercise to show that equations (45), which now take the form

$$\sum_i \boldsymbol{v}_i \cdot \mathrm{d}\tilde{\boldsymbol{P}}_i + \mathrm{d}\tilde{E}_i = 0 \qquad \sum_i \mathrm{d}\tilde{\boldsymbol{P}}_i = 0 \tag{54}$$

are exactly satisfied, due to the symmetries (49). In this way, the postulated noises exactly conserve momentum and energy.

A. Deterministic equations

The derivatives of the entropy function are

$$\frac{\partial S}{\partial x} \to \begin{pmatrix} -\frac{\mu_j}{T_j} \\ 0 \\ \frac{1}{T_j} \end{pmatrix} \tag{55}$$

where we have defined the chemical potential per unit mass μ_i and temperature T_i according to the usual definitions,

$$\frac{\mu_i}{T_i} = -\left.\frac{\partial S_i}{\partial M_i}\right|_{E,\mathcal{V}} \qquad \frac{1}{T_i} = \left.\frac{\partial S_i}{\partial E_i}\right|_{M,\mathcal{V}}. \tag{56}$$

According to theorem (44), the matrix M is given by

$$M \to \mathbf{M}_{ij} = \begin{pmatrix} 0 & \mathbf{0}^T & 0 \\ \mathbf{0} & \frac{\mathrm{d}\tilde{\boldsymbol{P}}_i\,\mathrm{d}\tilde{\boldsymbol{P}}_j^T}{2k_B\,\mathrm{d}t} & \frac{\mathrm{d}\tilde{\boldsymbol{P}}_i\,\mathrm{d}\tilde{E}_j}{2k_B\,\mathrm{d}t} \\ 0 & \frac{\mathrm{d}\tilde{E}_i\,\mathrm{d}\tilde{\boldsymbol{P}}_j^T}{2k_B\,\mathrm{d}t} & \frac{\mathrm{d}\tilde{E}_i\,\mathrm{d}\tilde{E}_j}{2k_B\,\mathrm{d}t} \end{pmatrix}. \tag{57}$$

The elements of the matrix M are obtained by using the definitions (47) and the property (51). The result is

$$\begin{aligned}
\frac{\mathrm{d}\tilde{\boldsymbol{P}}_i^\alpha \mathrm{d}\tilde{\boldsymbol{P}}_j^\beta}{\mathrm{d}t} &= \delta_{ij}\left[\sum_k \frac{B_{ik}^2}{2}\left(\delta^{\alpha\beta} + \boldsymbol{e}_{ik}^\alpha \cdot \boldsymbol{e}_{ik}^\beta\right)\right] - \frac{B_{ij}^2}{2}\left(\delta^{\alpha\beta} + \boldsymbol{e}_{ij}^\alpha \cdot \boldsymbol{e}_{ij}^\beta\right) \\
\frac{\mathrm{d}\tilde{\boldsymbol{P}}_i^\alpha \mathrm{d}\tilde{E}_j}{\mathrm{d}t} &= -\delta_{ij}\left[\sum_k \frac{B_{ik}^2}{2}\left(\frac{\boldsymbol{v}_{ik}^\alpha}{2} + \boldsymbol{e}_{ik}\cdot\frac{\boldsymbol{v}_{ik}}{2}\boldsymbol{e}_{ik}^\alpha\right)\right] - \frac{B_{ij}^2}{2}\left(\frac{\boldsymbol{v}_{ij}^\alpha}{2} + \boldsymbol{e}_{ij}\cdot\frac{\boldsymbol{v}_{ij}}{2}\boldsymbol{e}_{ij}^\alpha\right) \\
\frac{\mathrm{d}\tilde{E}_i \mathrm{d}\tilde{\boldsymbol{P}}_j^\alpha}{\mathrm{d}t} &= -\delta_{ij}\left[\sum_k \frac{B_{ik}^2}{2}\left(\frac{\boldsymbol{v}_{ik}^\alpha}{2} + \boldsymbol{e}_{ik}\cdot\frac{\boldsymbol{v}_{ik}}{2}\boldsymbol{e}_{ik}^\alpha\right)\right] + \frac{B_{ij}^2}{2}\left(\frac{\boldsymbol{v}_{ij}^\alpha}{2} + \boldsymbol{e}_{ij}\cdot\frac{\boldsymbol{v}_{ij}}{2}\boldsymbol{e}_{ij}^\alpha\right) \\
\frac{\mathrm{d}\tilde{E}_i \mathrm{d}\tilde{E}_j}{\mathrm{d}t} &= \delta_{ij}\left[\sum_k \frac{B_{ik}^2}{2}\left(\left(\frac{\boldsymbol{v}_{ik}}{2}\right)^2 + \left(\boldsymbol{e}_{ik}\cdot\frac{\boldsymbol{v}_{ik}}{2}\right)^2\right)\right] \\
&\quad + \frac{B_{ij}^2}{2}\left(\left(\frac{\boldsymbol{v}_{ij}}{2}\right)^2 + \left(\boldsymbol{e}_{ij}\cdot\frac{\boldsymbol{v}_{ji}}{2}\right)^2\right) + \delta_{ij}\sum_k C_{ik}^2 - C_{ij}.
\end{aligned} \tag{58}$$

We are now in a position to write the deterministic irreversible part of the dynamics $\dot{x}|_{\mathrm{irr}} = M\frac{\partial S}{\partial x}$, which will be given by

$$\begin{pmatrix} \dot{M}_i \\ \dot{\boldsymbol{P}}_i \\ \dot{E}_i \end{pmatrix}_{|\mathrm{irr}} = \sum_j \mathbf{M}_{ij} \begin{pmatrix} -\frac{\mu_j}{T_j} \\ \mathbf{0} \\ \frac{1}{T_j} \end{pmatrix}. \tag{59}$$

The matrix multiplication leads readily to the following equations

$$\begin{aligned}
\dot{M}_i|_{\mathrm{irr}} &= 0 \\
\dot{\boldsymbol{P}}_i|_{\mathrm{irr}} &= -\sum_j a_{ij}(\boldsymbol{v}_{ij} + \boldsymbol{e}_{ij}\cdot\boldsymbol{v}_{ij}\boldsymbol{e}_{ij}) \\
\dot{E}_i|_{\mathrm{irr}} &= -\sum_j c_{ij}(T_i - T_j) + \frac{1}{2}\sum_j a_{ij}\left(\boldsymbol{v}_{ij}^2 + (\boldsymbol{v}_{ij}\cdot\boldsymbol{e}_{ij})^2\right)
\end{aligned} \tag{60}$$

where we have introduced the following quantities

$$a_{ij} = \frac{B_{ij}^2}{8k_B}\left(\frac{1}{T_i} + \frac{1}{T_j}\right) \qquad c_{ij} = \frac{C_{ij}^2}{2k_B T_i T_j}. \tag{61}$$

If we make the assumptions

$$a_{ij} = \eta\frac{A_{ij}}{R_{ij}} \qquad c_{ij} = \lambda\frac{A_{ij}}{R_{ij}} \tag{62}$$

where η is the bulk viscosity, λ the thermal conductivity and A_{ij} the area of the face i, j, the final deterministic irreversible part of the dynamics (60) becomes

$$\begin{aligned}
\dot{M}_i|_{\mathrm{irr}} &= 0 \\
\dot{\boldsymbol{P}}_i|_{\mathrm{irr}} &= -\eta\sum_j \frac{A_{ij}}{R_{ij}}(\boldsymbol{v}_{ij} + \boldsymbol{v}_{ij}\cdot\boldsymbol{e}_{ij}\boldsymbol{e}_{ij}) \\
\dot{E}_i|_{\mathrm{irr}} &= -\sum_j \lambda\frac{A_{ij}}{R_{ij}}(T_i - T_j) + \frac{\eta}{2}\sum_j \frac{A_{ij}}{R_{ij}}\left((\boldsymbol{v}_{ij}\cdot\boldsymbol{e}_{ij})^2 + \boldsymbol{v}_{ij}^2\right).
\end{aligned} \tag{63}$$

These equations are *identical* to those obtained in [5] except for the presence in [5] of a term describing the advection of kinetic energy between cells. This term is very small as it is of

third order in $\boldsymbol{v}_{ij}$ as compared to the second-order terms in the rest of the energy equation. In the continuum limit where $\boldsymbol{v}_{ij}$ is replaced by gradients in velocity such higher order terms are discarded. Note that the second equation in (62) is basically the requirement that the bulk viscosity $\zeta = 2\eta/D$, an assumption made in [5]. Of course, this restriction can be relaxed if desired.

From equations (61) and (62), the functions B_{ij}, C_{ij} are given by

$$B_{ij} = \left(8k_B\eta\frac{T_iT_j}{T_i+T_j}\frac{A_{ij}}{R_{ij}}\right)^{1/2} \qquad C_{ij} = \left(2k_B\lambda T_iT_j\frac{A_{ij}}{R_{ij}}\right)^{1/2}. \tag{64}$$

B. Stochastic equations

We are still not done, because in order to write the correct Itô stochastic equations $\mathrm{d}x|_{\mathrm{irr}} = M\frac{\partial S}{\partial x} + k_B\frac{\partial M}{\partial x} + \mathrm{d}\tilde{x}$, we need to compute the term $k_B\frac{\partial M}{\partial x}$. This term can be understood essentially as coming from the stochastic interpretation selected, which is the Itô interpretation.

The derivatives of the matrix M are explicitly written as

$$\sum_j \frac{\partial}{\partial x_j}\mathbf{M}_{ij} = \sum_j \begin{pmatrix} 0 \\ \sum_j \frac{\partial}{\partial \boldsymbol{P}_j}\frac{\mathrm{d}\tilde{\boldsymbol{P}}_i\mathrm{d}\tilde{\boldsymbol{P}}_j}{2k_B\mathrm{d}t} + \sum_j \frac{\partial}{\partial E_j}\frac{\mathrm{d}\tilde{\boldsymbol{P}}_i\mathrm{d}\tilde{E}_j}{2k_B\mathrm{d}t} \\ \sum_j \frac{\partial}{\partial \boldsymbol{P}_j}\frac{\mathrm{d}\tilde{E}_i\mathrm{d}\tilde{\boldsymbol{P}}_j}{2k_B\mathrm{d}t} + \sum_j \frac{\partial}{\partial E_j}\frac{\mathrm{d}\tilde{E}_i\mathrm{d}\tilde{E}_j}{2k_B\mathrm{d}t} \end{pmatrix}. \tag{65}$$

By using the results (58) it is easy to compute the above derivatives.

$$\begin{aligned}
&k_B\sum_j \frac{\partial}{\partial \boldsymbol{P}_j}\frac{\mathrm{d}\tilde{\boldsymbol{P}}_i\mathrm{d}\tilde{\boldsymbol{P}}_j}{2k_B\mathrm{d}t} = 0 \\
&k_B\sum_j \frac{\partial}{\partial E_j}\frac{\mathrm{d}\tilde{\boldsymbol{P}}_i\mathrm{d}\tilde{E}_j}{2k_B\mathrm{d}t} = -\eta\sum_j \frac{A_{ij}}{R_{ij}}d_{ij}(\boldsymbol{v}_{ij} + \boldsymbol{v}_{ij}\cdot\boldsymbol{e}_{ij}\boldsymbol{e}_{ij}) \\
&k_B\sum_j \frac{\partial}{\partial \boldsymbol{P}_j}\frac{\mathrm{d}\tilde{E}_i\mathrm{d}\tilde{\boldsymbol{P}}_j}{2k_B\mathrm{d}t} = (D+1)k_B\sum_j \frac{A_{ij}}{R_{ij}}\left(\frac{T_iT_j}{T_i+T_j}\right)\left(\frac{1}{M_i}+\frac{1}{M_j}\right) \\
&k_B\sum_j \frac{\partial}{\partial E_j}\frac{\mathrm{d}\tilde{E}_i\mathrm{d}\tilde{E}_j}{2k_B\mathrm{d}t} = \frac{\eta}{2}\sum_j \frac{A_{ij}}{R_{ij}}d_{ij}\left((\boldsymbol{v}_{ij}\cdot\boldsymbol{e}_{ij})^2 + \boldsymbol{v}_{ij}^2\right) + \lambda\sum_j \frac{A_{ij}}{R_{ij}}\left[\frac{k_BT_j}{C_i} - \frac{k_BT_i}{C_j}\right]
\end{aligned} \tag{66}$$

where we have introduced

$$d_{ij} = \frac{1}{(T_i+T_j)^2}\left[\frac{T_j^2k_B}{C_i} + \frac{T_i^2k_B}{C_j}\right]. \tag{67}$$

Note that d_{ij} is a dimensionless quantity involving the heat capacity at constant volume of mesoparticle i, C_i. For mesoscopic particles, k_B/C_i is a small quantity.

Finally, the irreversible stochastic differential equation $\mathrm{d}x|_{\mathrm{irr}} = M\frac{\partial S}{\partial x}\,\mathrm{d}t + k_B\frac{\partial M}{\partial x}\,\mathrm{d}t + \mathrm{d}\tilde{x}$ becomes

$$\begin{aligned}
&\mathrm{d}M_i|_{\mathrm{irr}} = 0 \\
&\mathrm{d}\boldsymbol{P}_i|_{\mathrm{irr}} = -\eta\sum_j \frac{A_{ij}}{R_{ij}}(1+d_{ij})\left(\boldsymbol{v}_{ij} + \boldsymbol{e}_{ij}\cdot\boldsymbol{v}_{ij}\boldsymbol{e}_{ij}\right)\mathrm{d}t + \mathrm{d}\tilde{\boldsymbol{P}}_i \\
&\mathrm{d}E_i|_{\mathrm{irr}} = -\sum_j \lambda\frac{A_{ij}}{R_{ij}}(T_i - T_j)\,\mathrm{d}t + \frac{\eta}{2}\sum_j \frac{A_{ij}}{R_{ij}}(1+d_{ij})\left((\boldsymbol{v}_{ij}\cdot\boldsymbol{e}_{ij})^2 + \boldsymbol{v}_{ij}^2\right)\mathrm{d}t - \lambda\sum_j \frac{A_{ij}}{R_{ij}} \\
&\qquad\times\left(\frac{k_BT_i}{C_j} - \frac{k_BT_j}{C_i}\right)\mathrm{d}t - (D+1)\eta k_B\sum_j \frac{A_{ij}}{R_{ij}}\frac{T_iT_j}{T_i+T_j}\left[\frac{1}{M_i}+\frac{1}{M_j}\right]\mathrm{d}t + \mathrm{d}\tilde{E}_i.
\end{aligned} \tag{68}$$

To leading order in k_B/C_i (which is typically the inverse number of atoms in the cell) these equations coincide with the corresponding equations in [5]. However, in [5] the terms proportional to d_{ij} and k_B/C_i are not present, as terms of relative order k_B/C_i are discarded throughout.

References

[1] Mazur P and Bedeaux D 1974 *Physica* **76** 235
[2] Landau L D and Lifshitz E M 1959 *Fluid Mechanics* (Oxford: Pergamon)
[3] Español P 1998 *Physica* A **248** 77
[4] Eulerian implementations of fluctuating hydrodynamics have been considered by Garcia A L, Mansour M M, Lie G C and Clementi E 1987 *J. Stat. Phys.* **47** 209
Breuer H-P and Petruccione F 1993 *Physica* A **192** 569
[5] Flekkøy E G and Coveney P V 1999 *Phys. Rev. Lett.* **83** 1775
Flekkøy E G, Coveney P V and De Fabritiis G 2000 *Phys. Rev.* E **62** 2140
De Fabritiis G, Coveney P V and Flekkøy E G 2001 *Phil. Trans. R. Soc.* A at press
[6] Serrano M and Español P 2001 *Phys. Rev.* E **64** 046115
[7] Español P 1995 *Phys. Rev.* E **52** 1734
[8] Grmela M and Öttinger H C 1997 *Phys. Rev.* E **56** 6620
Öttinger H C and Grmela M 1997 *Phys. Rev.* E **56** 6633
Öttinger H C 1998 *Phys. Rev.* E **57** 1416
Öttinger H C 1997 *J. Non-Equilib Thermodyn* **22** 386
Öttinger H C 1998 *Physica* A **254** 433
[9] Avalos J B and Mackie A D 1997 *Europhys. Lett.* **40** 141
[10] Hoogerbrugge P J and Koelman J M V A 1992 *Europhys. Lett.* **19** 155
Español P and Warren P 1995 *Europhys. Lett.* **30** 191
[11] Español J and de la Rubia F J 1992 *Physica* A **187** 589
[12] Weaire D, Kermode J P and Wejchert J 1986 *Phil. Mag.* B **53** L101
[13] Callen H B 1960 *Thermodynamics* (New York: Wiley)
[14] Español P 2001 *J. Chem. Phys.* **115** 5392
[15] Computational Geometry Algorithms Library, http://www.cgal.org